



Involvement of NADPH Oxidase 1 in Liver Kinase B1-Mediated Effects on Tumor Angiogenesis and Growth

Elisabetta Zulato¹, Francesco Ciccarese², Giorgia Nardo¹, Marica Pinazza¹,
Valentina Agnusdei¹, Micol Silic-Benussi¹, Vincenzo Ciminale^{1,2} and Stefano Indraccolo^{1*}

¹Istituto Oncologico Veneto IOV – IRCCS, Padova, Italy, ²Department of Surgery, Oncology and Gastroenterology, University of Padova, Padova, Italy

OPEN ACCESS

Edited by:

Giuseppe Filomeni,
Danish Cancer Society, Denmark

Reviewed by:

Alfredo Criollo,
Universidad de Chile, Chile
Zhi-Xiang Xu,
University of Alabama at Birmingham,
United States

*Correspondence:

Stefano Indraccolo
stefano.indraccolo@unipd.it

Specialty section:

This article was submitted to
Molecular and Cellular Oncology,
a section of the journal
Frontiers in Oncology

Received: 09 February 2018

Accepted: 14 May 2018

Published: 04 June 2018

Citation:

Zulato E, Ciccarese F, Nardo G,
Pinazza M, Agnusdei V, Silic-
Benussi M, Ciminale V and
Indraccolo S (2018) Involvement of
NADPH Oxidase 1 in Liver Kinase
B1-Mediated Effects on Tumor
Angiogenesis and Growth.
Front. Oncol. 8:195.
doi: 10.3389/fonc.2018.00195

The liver kinase B1 (LKB1) gene is a tumor suppressor with an established role in the control of cell metabolism and oxidative stress. However, whether dis-regulated oxidative stress promotes growth of LKB1-deficient tumors remains substantially unknown. Through *in vitro* studies, we observed that loss of LKB1 perturbed expression of several genes involved in reactive oxygen species (ROS) homeostasis. In particular, this analysis evidenced strongly up-modulated NADPH oxidase 1 (NOX1) transcript levels in tumor cells lacking LKB1. NOX1 accounted in part for enhanced cytotoxic effects of H₂O₂-induced oxidative stress in A549 LKB1-deficient tumor cells. Notably, genetic and pharmacologic inhibition of NOX1 activity reduced angiogenesis and growth of A549 tumors in mice. These results suggest that NOX1 inhibitors could counteract ROS production and the angiogenic switch in LKB1-deficient tumors.

Keywords: NADPH oxidase 1, liver kinase B1, angiogenesis, lung cancer, reactive oxygen species, oxidative stress

INTRODUCTION

Increased oxidative stress is common in cancer cells. In fact, uncontrolled proliferation is connected with profound metabolic remodeling accompanied by altered redox status. Reactive oxygen species (ROS) are important biological messengers involved in cell signaling, tumor growth, and metastasis (1). Recent studies suggest that increased oxidative stress could be exploited for therapeutic purposes (2, 3), as tumor cells might be particularly vulnerable to drugs which further increase oxidative stress or otherwise block biochemical buffers of ROS (4).

The liver kinase B1 (LKB1) is a serine threonine kinase, whose hereditary mutations are associated with the Peutz-Jeghers syndrome and is somatically mutated or deleted in certain tumor types, with relatively high frequencies in non-small cell lung cancer (NSCLC) and cervical carcinoma (5). LKB1 is involved in energy homeostasis control, as well as control of cell proliferation and polarity (6). LKB1 and its downstream effector AMP-activated protein kinase (AMPK) have also been recently involved in metabolic adaptation and in the regulation of tumor cell response to oxidative stress by various mechanisms including control of NADPH homeostasis (7) and enhancement of the activity of superoxide dismutase-2 and catalase by a p38-mediated mechanism (8). These studies largely utilized LKB1-deficient tumor cell lines and their matched LKB1-proficient counterpart to

Abbreviations: LKB1, liver kinase B1; NOX1, NADPH oxidase 1; ROS, reactive oxygen species; NSCLC, non-small cell lung cancer; AMPK, AMP-activated protein kinase; ACC, acetyl-CoA carboxylase; CCLE, cancer cell line encyclopedia; NAC, N-acetyl cysteine; MVD, microvessel density; NRF2, nuclear respiratory factor 2; bFGF, basic fibroblast growth factor; VEGF, vascular endothelial growth factor; VEGFR, vascular endothelial growth factor receptor.

investigate effects of this kinase on oxidative stress. Although several features and mechanisms associated with altered ROS homeostasis in LKB1-mutant tumor cells have been uncovered by using this experimental system, previous studies did not analyze the transcriptional perturbations of genes involved in redox control in LKB1-deficient cell lines.

Here, we investigated at transcriptional level three pairs of LKB1-deficient cell lines and observed that LKB1 is involved in the regulation of NADPH oxidase 1 (*NOX1*) transcript expression. Inhibition of *NOX1* activity attenuated cytotoxic effects of oxidative stress in LKB1-deficient tumor cells *in vitro* and was an effective strategy to prevent the angiogenic switch and growth of LKB1-deficient A549 tumors *in vivo*. Although marked heterogeneity in the expression levels of *NOX1* among LKB1-deficient lung and cervical cancer cell lines does not allow us to generalize these findings, our results hint at *NOX1* as a candidate mediator of angiogenesis in a subset of LKB1-deficient tumors.

MATERIALS AND METHODS

Cell Culture and *In Vitro* Treatments

A549 cells were provided by Dr. Reuben J. Shaw (Salk Institute for Biological Studies, La Jolla, CA, USA). H460, H1650, H1975, HeLa, SiHa, and HEK293T cells were purchased from ATCC (Manassas, VA, USA). H23, H1437, H2228, H2009, and H1299 cell lines were kindly provided by Dr. Massimo Broggin (Mario Negri Institute, Milan, Italy). HeLa, SiHa, and HEK293T cells were cultured in Dulbecco modified Eagle medium (DMEM; EuroClone, Milan, Italy), supplemented with 10% FCS (EuroClone), 10 mM HEPES, and 1% antibiotic-antimycotic mix (Thermo Fisher, Waltham, MA, USA). H460, H1650, H1975, H23, H1437, H2228, H2009, and H1299 cells were grown in RPMI1640 medium (EuroClone) supplemented with 10% FCS, 1% HEPES, 1% Na pyruvate, 2 mM L-Glutamine (Lonza, Basel, Switzerland), and 1% antibiotic-antimycotic mix. A549 cells were cultured in DMEM-F12 medium (Gibco-BRL, Grand Island, NY, USA) supplemented with 10% FCS, 2 mM L-Glutamine, and 1% antibiotic-antimycotic mix. In some experiments, cell lines were treated with the appropriate vehicle or with the following substances: 2 mM hydrogen peroxide (H₂O₂, Sigma-Aldrich, Saint Luis, MO, USA), 2 mM N-acetylcysteine (NAC, Sigma-Aldrich), 100 μM apocynin (Sigma-Aldrich), for the indicated time points.

Retrovirus Production and Transduction With Viral Particles

The retroviral vector overexpressing human LKB1^{wt} (RV-LKB1^{wt}; plasmid # 8592) and the corresponding control vector (pBabe, plasmid # 1764) used to transduce LKB1-mutated cells were purchased from Addgene (Cambridge, MA, USA). Viral particles were produced by transfecting HEK293T cells with second-generation packaging plasmids. Virus was harvested 24 and 48 h after transfection and concentrated by ultracentrifugation at 24,000 rpm for 2 h. A549, H460, and HeLa cells were transduced with a VSV-G-pseudotyped retroviral vector encoding LKB1 cDNA (LKB1^{wt}) or with an empty vector (pBabe). Briefly, 0.5 × 10⁶ cells were incubated at 37°C overnight and 200 μl of concentrated vector-containing supernatant were layered over target cells.

The day after, cells were washed and cultured in fresh medium. Cells expressing the constructs were selected in puromycin-containing medium (8 μg/ml for A549 and H460 cells, 4 μg/ml for HeLa cells) for 10–14 days prior to subsequent analysis.

Reverse Transcription-PCR and Quantitative PCR

Total RNA was isolated using RNAeasy[®] Mini Kit (Qiagen, Venlo, Netherlands) according to manufacturer's instructions. cDNA was synthesized from 0.3 to 1 μg of total RNA using High Capacity RNA-to-cDNA Kit (Thermo Fisher). Expression levels of 20 oxidative metabolism-related genes were analyzed by real-time Ready custom panels (Roche Diagnostics, Basel, Switzerland). Real-time PCRs were performed using Platinum[®] SYBR[®] Green (Thermo Fisher) in an ABI Prism 7900 HT Sequence Detection System (Thermo Fisher). Results were analyzed using the ΔΔCt method with normalization against HMBS gene expression.

Genes included in Custom Panels were selected based on their role in oxidative metabolism and are reported in **Table 1**. Primers used for qRT-PCR are reported in **Table 2**.

TABLE 1 | Genes included in custom panel.

Gene ID	Description	HGNC ID	Pathway
<i>GCLC</i>	Glutamate-cysteine ligase, catalytic subunit	4311	
<i>GCLM</i>	Glutamate-cysteine ligase, modifier subunit	4312	Glutathione synthesis
<i>GSS</i>	Glutathione synthetase	4624	
<i>GGT6</i>	Gamma-glutamyltransferase 6	26891	Glutathione degradation
<i>GGT7</i>	Gamma-glutamyltransferase 7	4259	
<i>NFE2L2</i>	Nuclear factor erythroid 2-like 2; nuclear respiratory factor 2	7782	Transcription factors involved in glutathione metabolism
<i>JUN</i>	<i>jun</i> proto-oncogene	6204	
<i>ABCC1</i>	ATP-binding cassette sub-family C member 1	51	Glutathione adducts transporters
<i>ABCC2</i>	ATP-binding cassette sub-family C member 2	53	
<i>CAT</i>	Catalase	1516	
<i>TXN</i>	Thioredoxin	12435	Enzymes involved in antioxidant defenses
<i>SOD2</i>	Superoxide dismutase-2	11180	
<i>GPX1</i>	Glutathione peroxidase 1	4353	
<i>GSR</i>	Glutathione reductase	4623	
<i>MSRA</i>	Methionine sulfoxide reductase A	7377	
<i>NOX1</i>	NADPH oxidase 1	7889	Enzymes involved in reactive oxygen species production
<i>CBS</i>	Cystathionine β-synthase	1550	Enzymes involved in transsulfuration pathway
<i>CTH</i>	Cystathionine γ-lyase	2505	
<i>SLC7A11</i>	Solute carrier family 7 member 11; xCT	11059	
<i>SLC7A10</i>	Solute carrier family 7 member 10; ASC1	11058	Cystine and cysteine transporters
<i>HMBS</i>	Hydroxymethylbilane synthase	4982	
<i>B2M</i>	Beta-2-microglobulin	914	Reference gene
<i>ACTB</i>	Actin, beta	132	

TABLE 2 | Primers used for qRT-PCR.

Gene ID	Forward primer	Reverse primer
<i>NADPH oxidase 1</i>	5'-GGGGTCAAACAGAG GAGAGC-3'	5'-CCACTTCCAAGACT CAGGGG-3'
<i>HMBS</i>	5'-GGCAATGCGGCTGCAA-3'	5'-GGGTACCCACGCGA ATCAC-3'

Annexin-V/Propidium Iodide Assay

Cells were incubated with Annexin-V-FITC in HEPES buffer containing propidium iodide (PI), using the Annexin-V Fluos Staining Kit (Roche Diagnostics, Mannheim, Germany). Labeled cells were analyzed on EPICS-XL cytofluorimeter using Expo32 software (Beckman Coulter, Fullerton, CA, USA). Dot plot images were obtained by using the Kalusa analysis 1.3 software (Beckman Coulter).

Measurement of Mitochondrial Membrane Potential ($\Delta\psi$)

Cells were incubated with tissue culture medium containing 15 nM tetramethylrhodamine, methyl ester (TMRM; Thermo Fisher) and 20 ng/ml Verapamil (efflux pumps inhibitor; Sigma-Aldrich) for 15 min at room temperature. Labeled cells were analyzed with an LSRII flow cytometer using the 560 nm laser and the 585/15 nm filter.

RNAi Experiments

Cells (3×10^5) were seeded in six-well tissue culture plates. The following day, Opti-MEM[®] I Medium with GlutaMAX[™] (Thermo Fisher) was mixed separately with 20 nM Stealth RNAi[™] siRNA (Thermo Fisher) and with Lipofectamine[®] RNAiMAX Transfection Reagent (Thermo Fisher) and incubated 5 min at room temperature. Separated mix were combined and, following additional 20 min of incubation, 500 μ l of final mix were added, drop by drop, to adherent cells, along with 1.5 ml of culture medium. Lipofection was blocked after 6 h, through removal of medium with liposomes and addition of culture medium. Sequences of Stealth RNAi[™] siRNAs are reported in **Table 3**.

In Vivo Experiments

Procedures involving animals and their care conformed to institutional guidelines that comply with national and international laws and policies (EEC Council Directive 86/609, OJ L 358, 12 December, 1987) and were authorized by the ethical committee of the University of Padova and the Italian Ministry of Health (Authorization no. 143/2012-B). For tumor establishment, both dorsolateral flanks of 8-week-old SCID mice (Charles River, Wilmington, MA, USA) were injected subcutaneously with 0.5×10^6 LKB1^{mut} A549 tumor cells mixed at 4°C with liquid Matrigel (Becton-Dickinson). Tumor volume (mm³) was measured by caliber and calculated according to the following formula: $L \times l^2 \times 0.5$, where L is the longest diameter, l is the shortest diameter, and 0.5 is a constant to calculate the volume of an ellipsoid. In the experiment with NAC, LKB1^{mut} A549 cells were 16 h pretreated with NAC 2 mM before injection and during tumor growth NAC was administered intraperitoneally

TABLE 3 | Stealth siRNAs used in transfection experiments.

Stealth siRNA name	Stealth siRNA code	Sense sequence
siRNA	Negative Control Low GC Duplex	AGCUACACUAUCGAGCAAUUAACUU
siNOX1	NOX1HSS178287	UGGGAUGAUCGUGACUCCACUGUA

at 150 mg/kg every day. Control mice received intraperitoneal injections of PBS. In the experiment in which expression level of NOX1 was reduced by siRNA-mediated silencing, LKB1^{mut} A549 cells were injected 48 h after lipofection. In the experiment with apocynin, LKB1^{mut} A549 cells were 16 h pretreated with apocynin at 100 μ M before injection and during tumor growth apocynin was administered *via* oral gavage at 16 mg/kg every day.

At the end of the experiment, mice were killed by cervical dislocation. For all experiments, five to six mice per group were used. The tumors were harvested by dissection and snap-frozen.

Immunofluorescence Analysis (IFA)

Tumor vessels were labeled with a rat anti-CD31 mAb (1:50 dilution; Becton-Dickinson) followed by staining with a goat anti-rat 546 secondary antibody (Thermo Fisher). Sections of 5 μ m were cut from frozen biopsies and microvessel density (MVD) was quantified by screening the CD31-stained sections for the areas of highest vascularity, as previously reported (9). Briefly, nuclei were stained with TO-PRO-3 Iodide (1:1,000 dilution; Thermo Fisher). Immunofluorescence signals were visualized on a Zeiss Axiovert 100 M confocal microscope (Carl Zeiss AG; Oberkochen, Germany), using argon (488 nm) and helium-neon (543–633 nm) laser sources. For each sample, the number of fields analyzed varied between 5 and 10 per sample, depending on the size of sections; at least 4 samples per group were analyzed. Images were collected at a magnification of 200 \times . MVD was quantified by screening for the areas of highest vascularity. Two independent operators blindly evaluated the images: morphologically identifiable vessels were counted as an individual vessel.

Statistical Analysis

Results were expressed as mean value \pm SD. Student's *t*-test or Mann-Whitney test were used depending on the distribution of values. Differences were considered statistically significant when $P < 0.05$. For each cell line, data are expressed as fold change arbitrarily setting controls at 1. If not specified otherwise, the symbol § was used for comparison between LKB1^{mut} and LKB1^{wt} cells, the symbol * for comparison between treated and untreated cells and the symbol # for comparison between treated cells and cells pre-treated with other drugs (NAC, Apocynin) or siRNA.

RESULTS

LKB1 Regulates Expression of Genes Involved in ROS Metabolism in Tumor Cells

To investigate whether LKB1 modulated expression of genes involved in the response to cellular redox stress, we compared

expression levels of 20 relevant genes (Table 1) by real-time PCR in human tumor cell lines isogenic for LKB1 status and grown *in vitro* under standard conditions. We performed these experiments using the LKB1-deficient NSCLC cell lines A549 and H460, and cervical carcinoma cell line HeLa transduced with a control retroviral vector (hereafter referred to as LKB1^{mut}) and their LKB1-proficient counterparts obtained by retroviral transduction of wild-type LKB1 cDNA (hereafter referred to as LKB1^{wt}). As expected, LKB1 reconstitution fully restored AMPK and acetyl-CoA carboxylase phosphorylation under glucose starvation—a condition known to trigger LKB1-dependent AMPK activation and associated with oxidative stress [(10) and data not shown]. Remarkably, in all cell lines tested, several antioxidant genes were downregulated and others were upregulated following reconstitution of LKB1 (Figure 1). Most of these variations were, however, not shared by the various cell lines analyzed. The most consistently downregulated gene in LKB1^{wt} cells was *NOX1*, a homolog of the macrophage *NOX2*, accounting for the respiratory burst in response to pathogens (11). NADPH oxidases catalyze the transfer of one electron from NADPH to oxygen, generating superoxide or H₂O₂, thus further increasing oxidative stress (12).

Further analysis of *NOX1* mRNA levels in nine NSCLC and two cervical cancer cell lines, with known *LKB1* mutational status, showed that almost all cell lines bearing *LKB1* mutations presented increased *NOX1* expression compared with *LKB1* wild-type cells (Figure 2A). However, broad heterogeneity in *NOX1* expression was detected in LKB1-mutant cell lines, being *NOX1* levels particularly high in A549 cells (Figure 2A). An additional *in silico* analysis was performed by matching the *LKB1* mutational status and *NOX1* mRNA transcript data of tumor cell lines, available at the COSMIC and Cancer Cell Line Encyclopedia web sites, respectively. Results showed that *NOX1* transcripts were significantly increased in LKB1-mutated NSCLC cell lines, thus strengthening our observations (Figure 2B). The relatively high expression of *NOX1* in A549 cells led us to focus on these cells to investigate the possible involvement of *NOX1* in the regulation of oxidative stress.

NOX1 Accounts for Increased Sensitivity to Exogenous Oxidative Stress in A549 Cells

Gene silencing and pharmacologic inhibition approaches were used to analyze whether *NOX1* could account for increased sensitivity to oxidative stress in LKB1^{mut} cells. Interestingly, siRNA-mediated *NOX1* silencing in A549 cells increased resistance of LKB1^{mut} A549 cells to H₂O₂-induced cell death, while leaving substantially unaffected response to oxidative stress in LKB1^{wt} cells (Figure 3A). Consistent with this, measurement of mitochondrial membrane potential showed a significant increase in the number of TMRM negative LKB1^{mut} A549 cells upon H₂O₂-treatment (Figure 3B). This phenomenon in the mitochondrial membrane potential was partially rescued by *NOX1* silencing. Similar results were obtained following *NOX1* inhibition with apocynin (Figure 3C). It should be noted that despite interference with *NOX1* activity, LKB1^{mut} cells showed increased H₂O₂-induced cell death compared with LKB1^{wt} cells (Figures 3A–C), probably

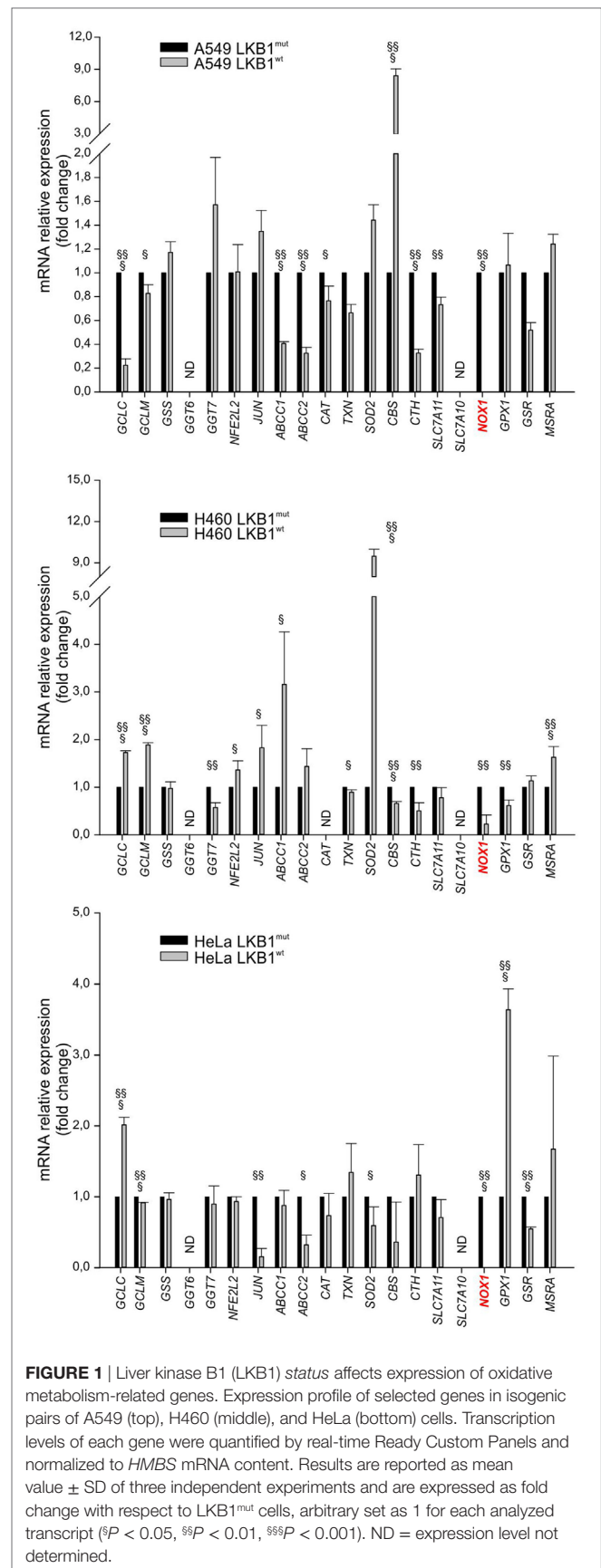


FIGURE 1 | Liver kinase B1 (*LKB1*) status affects expression of oxidative metabolism-related genes. Expression profile of selected genes in isogenic pairs of A549 (top), H460 (middle), and HeLa (bottom) cells. Transcription levels of each gene were quantified by real-time Ready Custom Panels and normalized to *HIMBS* mRNA content. Results are reported as mean value \pm SD of three independent experiments and are expressed as fold change with respect to LKB1^{mut} cells, arbitrary set as 1 for each analyzed transcript (§*P* < 0.05, §§*P* < 0.01, §§§*P* < 0.001). ND = expression level not determined.

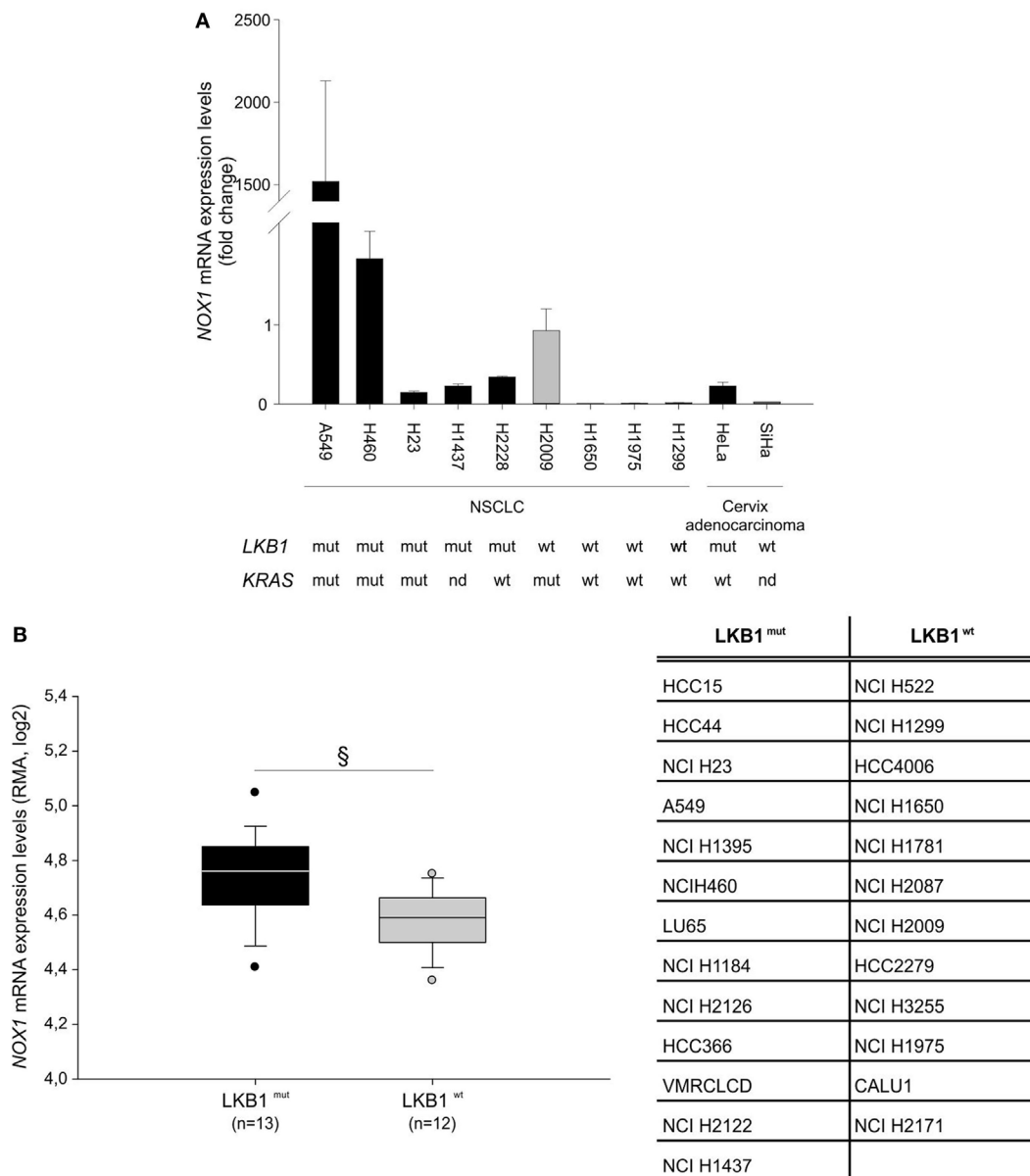


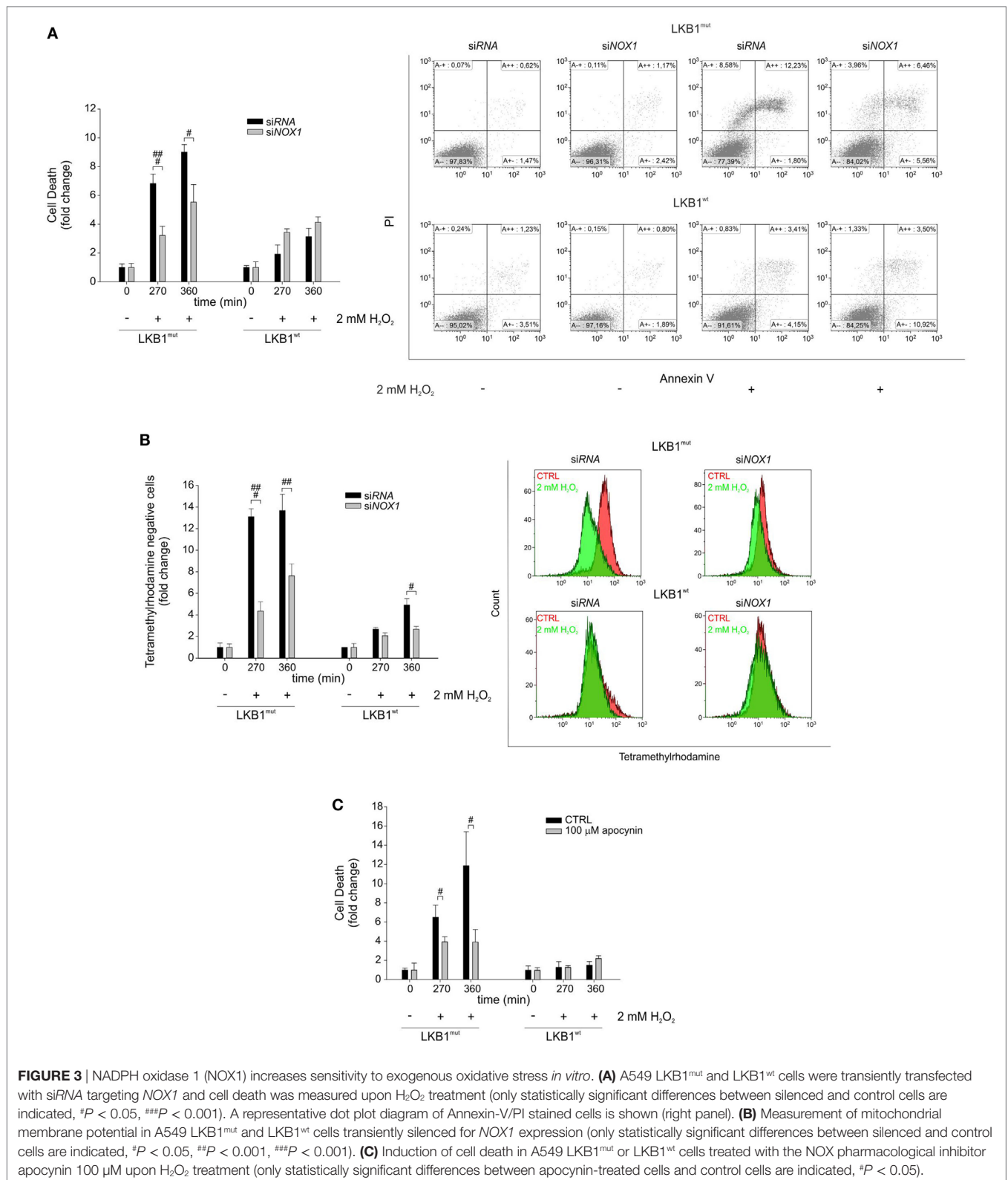
FIGURE 2 | Liver kinase B1 (LKB1) controls NADPH oxidase 1 (*NOX1*) expression in human cell lines. *NOX1* expression levels in LKB1-deficient (LKB1^{mut}) and LKB1-proficient (LKB1^{wt}) non-small cell lung cancer (NSCLC) and cervical cancer cell lines. **(A)** Expression levels of *NOX1* mRNA in NSCLC and cervical cancer cell lines, with defined *LKB1* and *KRAS* mutational status. Results are reported as mean value \pm SD of three independent experiments and are expressed as fold change compared to H2009 cells, arbitrary set at 1. **(B)** *In silico* analysis of *NOX1* levels in NSCLC cell lines. Expression level of *NOX1* as Robust Multi-array Average (RMA) values (source: Cancer Cell Line Encyclopedia). The dispersion of *NOX1* expression values in $n = 13$ LKB1 mutated and in $n = 12$ LKB1 wild-type cancer cell lines is represented as box-plots, indicating the first and the third quartiles and the median. The list of LKB1-mutated and non-mutated cancer cell lines is reported in the table ($^{\S}P < 0.05$). nd = mutational status not determined.

due to either incomplete blockade of NOX1 or multifactorial mechanisms of control of oxidative stress by LKB1.

NOX1 Promotes Angiogenesis and Growth of LKB1-Deficient A549 Tumors

High levels of ROS have been involved in induction of angiogenesis and tumor growth (13). To investigate whether oxidative stress

could play a role in LKB1^{mut} tumor formation, we co-injected LKB1^{mut} A549 cells along with administration of the antioxidant NAC. LKB1^{mut} A549 cells formed tumors (Figure 4A), and co-injection with NAC resulted in significant reduction of tumor growth and reduction of tumor vascularization, assessed 7 days after tumor cell injection (Figure 4A). Notably, chronic administration of apocynin significantly reduced tumor growth and MVD of LKB1^{mut} tumors (Figure 4A), suggesting that blockade of NOX



activity impairs angiogenesis and tumor growth. These results were confirmed and strengthened by siRNA-mediated silencing of NOX1 in A549 cells prior to their injection in mice (Figure 4B).

Analysis of expression levels of NOX1 in samples recovered 7 days after tumor cell injection showed, as expected, marginal silencing of the target gene, in contrast to the >80% reduction of NOX1

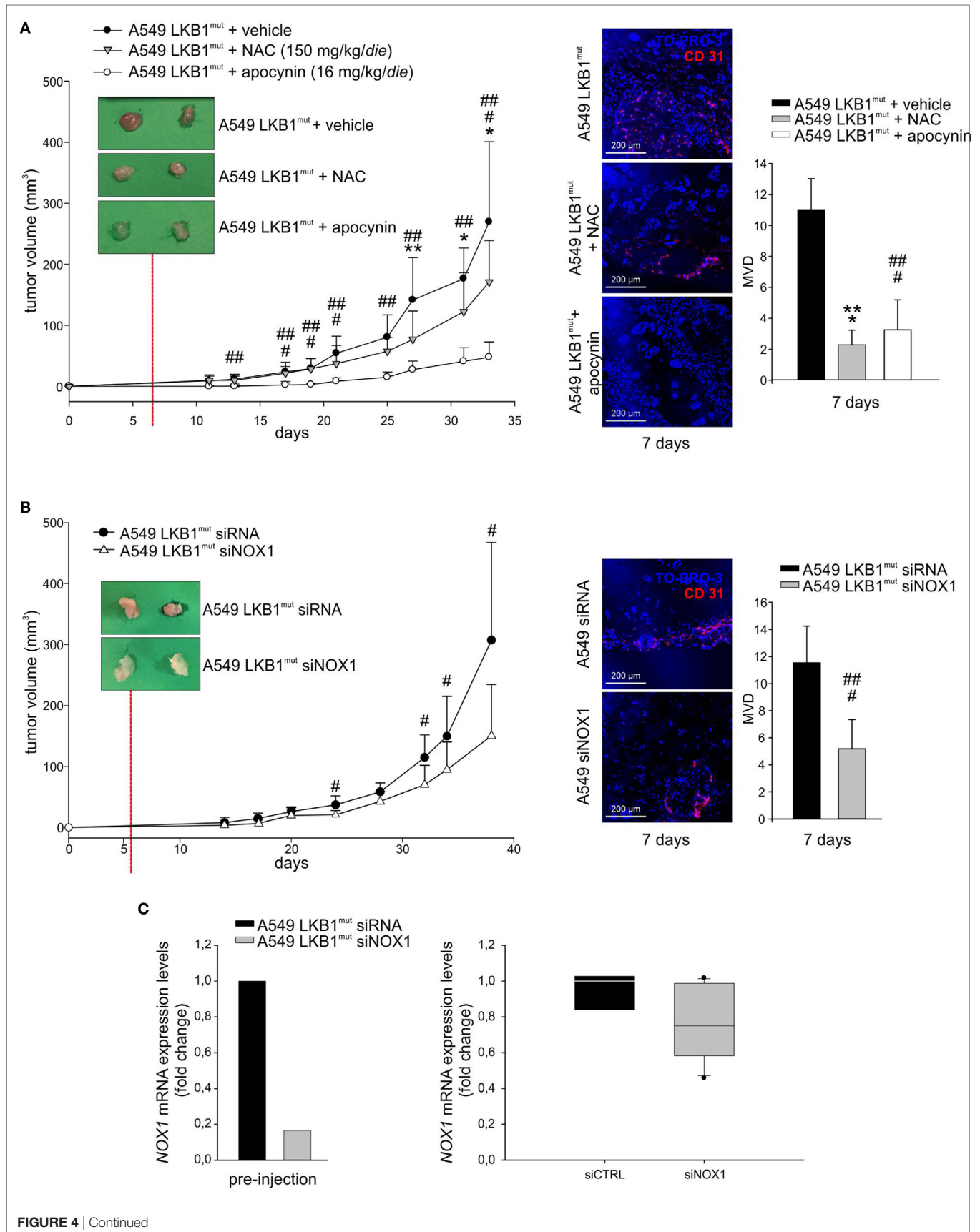


FIGURE 4 | NADPH oxidase 1 (NOX1) impacts on tumor growth and angiogenesis *in vivo*. **(A)** A549 LKB1^{mut} cells were s.c. injected in SCID mice and treated daily with either *N*-acetyl cysteine (NAC) (150 mg/kg/day, gray triangles), or apocynin (16 mg/kg/day, white dots), or vehicle (black dots) (left panel). The image of two representative masses/group shows a difference in vascularization of treated compared to untreated tumors 7 days after tumor cells injection, as indicated by CD31 staining (magnification 200×) and quantification of the microvessel density (MVD) (right panel) ($n = 3-6$ fields from five samples/group; * $P < 0.05$, ** $P < 0.01$, *** $P < 0.001$ A549 LKB1^{mut} NAC-treated versus untreated tumors; ** $P < 0.01$, *** $P < 0.001$ A549 LKB1^{mut} apocynin-treated versus untreated tumors). **(B)** Growth curves of s.c. tumors originated from A549 LKB1^{mut} cells transiently transfected with siRNA control (black dots) or with a siRNA targeting NOX1 (white triangles) (left panel). Seven days after tumor cells injection, LKB1^{mut} siRNA tumors appear more vascularized compared to LKB1^{mut} siNOX1 tumors, as shown by the representative image. Immunofluorescence analysis of CD31⁺ cells and quantification of microvasculature in tumors at day 7 (right panel) ($n = 3-6$ fields from five samples/group; * $P < 0.05$, *** $P < 0.001$ A549 LKB1^{mut} siRNA versus siNOX1). **(C)** Expression levels of NOX1 in LKB1-deficient (LKB1^{mut}) cells were analyzed prior to their injection in mice (bottom panel, at left) and in samples obtained from experiment shown in B ($n = 3$ and $n = 6$ for siRNA and siNOX1 samples, respectively) and recovered 1 week post injection (bottom panel, at right).

levels at time of injection (**Figure 4C**). This suggests that NOX1 could play a key role in the initial phases of the angiogenic switch in the A549 LKB1^{mut} tumor xenograft model.

DISCUSSION

This study disclosed for the first time an effect of LKB1 on NOX1 expression in tumor cells. According to our results, LKB1 acts as a suppressor of NOX1 expression at the RNA level. Among a set of 20 genes involved in redox homeostasis, NOX1 transcript was consistently down-regulated following forced expression of LKB1 cDNA in LKB1-deficient cancer cells. Other genes were also perturbed, presumably as a direct consequence of LKB1 loss or, alternatively, as adaptive response to compensate for loss of protective mechanisms. In this respect, Kaufman et al., reported that LKB1 loss leads to activation of the nuclear respiratory factor 2 transcription factor, which regulates oxidative stress response genes (14).

NADPH oxidase 1 belongs to a family of NADPH oxidase (11) and cancer cells generally express more NOX isoforms. In the case of A549 cells utilized in our study, NOX2 was expressed at a much lower baseline level compared to NOX1 and NOX4 was not expressed (data not shown). Therefore, although apocynin is not an isoform-selective NOX inhibitor (11), effects measured following treatment of A549 cells with this compound are likely to be accounted for by NOX1. A second consideration regards NOX1 levels in tumor cells. In fact, real-time PCR experiments showed marked differences in the relative expression levels of NOX1 among the NSCLC and cervical cancer cell lines analyzed (**Figure 2A**). It can, therefore, be speculated that the biological consequences of NOX1 inhibition might also depend on the amount of NOX1 in tumor cells. In line with this hypothesis, we indeed observed marked reduction of H₂O₂-induced cell death following apocynin treatment of A549 cells but not HeLa cells, which express substantially less NOX1 transcripts (**Figure 2** and data not shown). Therefore, although LKB1 acted as suppressor of NOX1 expression in all cell lines analyzed, other endogenous factors are likely to modulate NOX1 expression in tumor cells. According to previous studies, one of these factors could be KRAS, as its activating mutations were shown to correlate with NOX1 overexpression in human colon cancer samples (15) and in cancer cells (16). In this regard, analysis of NSCLC cancer cell lines showed increased NOX1 mRNA levels in cell lines bearing LKB1 and KRAS mutations (**Figure 2**). This heterogeneity may also have precluded the inclusion of NOX1 among top ranking

genes regulated by LKB1 in other genome-wide studies which previously investigated transcriptional profiles in LKB1-mutant cells and clinical samples (5, 14, 17, 18).

Although a detailed explanation of the mechanism connecting LKB1 to NOX1 is lacking and goes beyond the aim of our study, some hypothesis can be advanced. First, although LKB1 is not a transcription factor it is localized both in the cytoplasm and the nucleus of cells (17, 19). Therefore, suppression of NOX1 by LKB1 could be accounted for by its still poorly characterized nuclear functions. In this regard, it has been demonstrated that LKB1 forms a nuclear complex with the transcription regulatory factor LMO4, the transcription factor GATA-6 and Ldb1, and it has been suggested that this complex is involved in the regulation of GATA-mediated gene expression (20). Intriguingly, GATA-binding sites have been identified within the NOX1 promoter (21). It is thus possible that LKB1 could be involved in the regulation of NOX1 mRNA transcript through a GATA-6 mediated mechanism. Second, among indirect mechanisms, it has been shown that loss of LKB1 especially combined with KRAS mutations (as is the case in A549 cells) triggers the serine-glycine-one-carbon pathway, leading to increased S-adenosylmethionine generation, increased activity of DNA methyltransferases and elevation in DNA methylation (22). Hypothetically, this might silence some unknown repressor and thus unleash NOX1 expression. Hence, alterations of NOX1 expression might occur as consequence of changes in epigenetic marks following vector-mediated re-expression of LKB1 in tumor cells. Further studies are required to validate these hypothesis.

The second innovative observation of this study regards the anti-angiogenic effects of drugs affecting ROS homeostasis in the context of LKB1-deficient tumors. Previous studies reported a link between angiogenesis and LKB1 expression in tumor models. Zhuang et al. described reduction of MVD accompanied by reduced expression of the angiogenic factors basic fibroblast growth factor and vascular endothelial growth factor (VEGF) in LKB1-deficient MDA-MB435 xenografts when LKB1 cDNA was added back, but further mechanistic insights were not provided (23). Along this line, it was known that NOX1 can promote the angiogenic switch in NIH-3T3 fibroblasts converting them into tumorigenic cells by a mechanism involving generation of ROS and increased expression of VEGF mRNA (24). Therefore, in view of our findings, it is conceivable that some of the effects on VEGF expression that follow interventions on LKB1 might depend on modulation of NOX1 levels in tumor cells. Interestingly, Okon et al. reported that LKB1 functions as a

RAB7 effector and suppresses angiogenesis by promoting the cellular trafficking of neuropilin-1 from the RAB7 vesicles to the lysosomes for degradation (25). Neuropilin-1 is an angiogenic receptor that can be expressed both by endothelial and tumor cells (26). When expressed by tumor cells, neuropilin-1 seems to increase VEGF-mediated angiogenesis. Therefore, it can be speculated that adding LKB1 back to tumor cells triggers complex changes in the tumor microenvironment involving NOX1, ROS, and neuropilin-1 that impact on VEGF/VEGFR-2 signaling and angiogenesis with negative rebounds on tumor growth that largely exceed the modest effects on tumor cell proliferation, which can be detected *in vitro*. As the contribution of each component of this envisioned model could vary in individual tumors, additional studies are required to validate this hypothesis both in preclinical models and in patients.

In conclusion, our study disclosed for the first time that LKB1 controls *NOX1* expression *in vitro*. Perturbing ROS homeostasis or inhibition of NOX1 reduced tumor growth and angiogenesis *in vivo* and could represent a new possible therapeutic approach in LKB1-deficient KRAS-mutated tumors.

REFERENCES

- Panieri E, Santoro MM. ROS homeostasis and metabolism: a dangerous liaison in cancer cells. *Cell Death Dis* (2016) 7:e2253. doi:10.1038/cddis.2016.105
- Ciccarese F, Ciminale V. Escaping death: mitochondrial redox homeostasis in cancer cells. *Front Oncol* (2017) 7:117. doi:10.3389/fonc.2017.00117
- Raza MH, Siraj S, Arshad A, Waheed U, Aldakheel F, Alduraywish S, et al. ROS-modulated therapeutic approaches in cancer treatment. *J Cancer Res Clin Oncol* (2017) 143:1789–809. doi:10.1007/s00432-017-2464-9
- Gorrini C, Harris IS, Mak TW. Modulation of oxidative stress as an anticancer strategy. *Nat Rev Drug Discov* (2013) 12:931–47. doi:10.1038/nrd4002
- Ji H, Ramsey MR, Hayes DN, Fan C, Mcnamara K, Kozlowski P, et al. LKB1 modulates lung cancer differentiation and metastasis. *Nature* (2007) 448:807–10. doi:10.1038/nature06030
- Boudeau J, Sapkota G, Alessi DR. LKB1, a protein kinase regulating cell proliferation and polarity. *FEBS Lett* (2003) 546:159–65. doi:10.1016/S0014-5793(03)00642-2
- Jeon SM, Chandel NS, Hay N. AMPK regulates NADPH homeostasis to promote tumour cell survival during energy stress. *Nature* (2012) 485:661–5. doi:10.1038/nature11066
- Xu HG, Zhai YX, Chen J, Lu Y, Wang JW, Quan CS, et al. LKB1 reduces ROS-mediated cell damage via activation of p38. *Oncogene* (2015) 34:3848–59. doi:10.1038/nc.2014.315
- Trenti A, Zulato E, Pasqualini L, Indraccolo S, Bolego C, Trevisi L. Therapeutic concentrations of digitoxin inhibit endothelial focal adhesion kinase and angiogenesis induced by different growth factors. *Br J Pharmacol* (2017) 174:3094–106. doi:10.1111/bph.13944
- Spitz DR, Sim JE, Ridnour LA, Galoforo SS, Lee YJ. Glucose deprivation-induced oxidative stress in human tumor cells. A fundamental defect in metabolism? *Ann N Y Acad Sci* (2000) 899:349–62. doi:10.1111/j.1749-6632.2000.tb06199.x
- Altenhofer S, Radermacher KA, Kleikers PW, Winkler K, Schmidt HH. Evolution of NADPH oxidase inhibitors: selectivity and mechanisms for target engagement. *Antioxid Redox Signal* (2015) 23:406–27. doi:10.1089/ars.2013.5814
- Kamata T. Roles of Nox1 and other Nox isoforms in cancer development. *Cancer Sci* (2009) 100:1382–8. doi:10.1111/j.1349-7006.2009.01207.x
- Xia C, Meng Q, Liu LZ, Rojanasakul Y, Wang XR, Jiang BH. Reactive oxygen species regulate angiogenesis and tumor growth through vascular endothelial growth factor. *Cancer Res* (2007) 67:10823–30. doi:10.1158/0008-5472.CAN-07-0783

ETHICS STATEMENT

Procedures involving animals and their care conformed to institutional guidelines that comply with national and international laws and policies (EEC Council Directive 86/609, OJ L 358, 12 December, 1987) and were authorized by the ethical committee of the University of Padova and the Italian Ministry of Health (Authorization no. 143/2012-B).

AUTHOR CONTRIBUTIONS

SI conceived the study, designed experiments, analyzed data, and wrote the paper. EZ and FC designed and performed experiments, analyzed data, and wrote the paper. GN, MP, VA, and MS-B performed experiments and analyzed data. VC analyzed data and corrected the paper.

FUNDING

This work was supported by grants from the AIRC (IG18803 to SI).

- Kaufman JM, Amann JM, Park K, Arasada RR, Li H, Shyr Y, et al. LKB1 loss induces characteristic patterns of gene expression in human tumors associated with NRF2 activation and attenuation of PI3K-AKT. *J Thorac Oncol* (2014) 9:794–804. doi:10.1097/JTO.0000000000000173
- Laurent E, Mccoy JW III, Macina RA, Liu W, Cheng G, Robine S, et al. Nox1 is over-expressed in human colon cancers and correlates with activating mutations in K-Ras. *Int J Cancer* (2008) 123:100–7. doi:10.1002/ijc.23423
- Park MT, Kim MJ, Suh Y, Kim RK, Kim H, Lim EJ, et al. Novel signaling axis for ROS generation during K-Ras-induced cellular transformation. *Cell Death Differ* (2014) 21:1185–97. doi:10.1038/cdd.2014.34
- Jimenez AI, Fernandez P, Dominguez O, Dopazo A, Sanchez-Cespedes M. Growth and molecular profile of lung cancer cells expressing ectopic LKB1: down-regulation of the phosphatidylinositol 3'-phosphate kinase/PTEN pathway. *Cancer Res* (2003) 63:1382–8.
- Lin-Marq N, Borel C, Antonarakis SE. Peutz-Jeghers LKB1 mutants fail to activate GSK-3beta, preventing it from inhibiting Wnt signaling. *Mol Genet Genomics* (2005) 273:184–96. doi:10.1007/s00438-005-1124-y
- Nardo G, Favaro E, Curtarello M, Moserle L, Zulato E, Persano L, et al. Glycolytic phenotype and AMP kinase modify the pathologic response of tumor xenografts to VEGF neutralization. *Cancer Res* (2011) 71:4214–25. doi:10.1158/0008-5472.CAN-11-0242
- Setogawa T, Shinozaki-Yabana S, Masuda T, Matsuura K, Akiyama T. The tumor suppressor LKB1 induces p21 expression in collaboration with LMO4, GATA-6, and Ldb1. *Biochem Biophys Res Commun* (2006) 343:1186–90. doi:10.1016/j.bbrc.2006.03.077
- Adachi Y, Shibai Y, Mitsushita J, Shang WH, Hirose K, Kamata T. Oncogenic Ras upregulates NADPH oxidase 1 gene expression through MEK-ERK-dependent phosphorylation of GATA-6. *Oncogene* (2008) 27:4921–32. doi:10.1038/nc.2008.133
- Kottakis F, Nicolay BN, Roumane A, Karnik R, Gu H, Nagle JM, et al. LKB1 loss links serine metabolism to DNA methylation and tumorigenesis. *Nature* (2016) 539:390–5. doi:10.1038/nature20132
- Zhuang ZG, Di GH, Shen ZZ, Ding J, Shao ZM. Enhanced expression of LKB1 in breast cancer cells attenuates angiogenesis, invasion, and metastatic potential. *Mol Cancer Res* (2006) 4:843–9. doi:10.1158/1541-7786.MCR-06-0118
- Arbiser JL, Petros J, Klafter R, Govindajaran B, Mclaughlin ER, Brown LF, et al. Reactive oxygen generated by Nox1 triggers the angiogenic switch. *Proc Natl Acad Sci U S A* (2002) 99:715–20. doi:10.1073/pnas.022630199
- Okon IS, Coughlan KA, Zhang C, Moriasi C, Ding Y, Song P, et al. Protein kinase LKB1 promotes RAB7-mediated neuropilin-1 degradation to inhibit angiogenesis. *J Clin Invest* (2014) 124:4590–602. doi:10.1172/JCI75371

26. Miao HQ, Lee P, Lin H, Soker S, Klagsbrun M. Neuropilin-1 expression by tumor cells promotes tumor angiogenesis and progression. *FASEB J* (2000) 14:2532–9. doi:10.1096/fj.00-0250com

Conflict of Interest Statement: The authors declare that the research was conducted in the absence of any commercial or financial relationships that could be construed as a potential conflict of interest.

Copyright © 2018 Zulato, Ciccarese, Nardo, Pinazza, Agnusdei, Silic-Benussi, Ciminale and Indraccolo. This is an open-access article distributed under the terms of the Creative Commons Attribution License (CC BY). The use, distribution or reproduction in other forums is permitted, provided the original author(s) and the copyright owner are credited and that the original publication in this journal is cited, in accordance with accepted academic practice. No use, distribution or reproduction is permitted which does not comply with these terms.